High-Pressure Gas Injection in Carbonate Reservoirs: A Laboratory Investigation of Oil Displacement

Dairabay Abdeli
Satbayev University, Almaty, Kazakhstan
abdeli.dairabay@gmail.com

Han Dongsheng
CNLC International Kazakhstan Inc LLP, Almaty, Kazakhstan
handongsheng@cnlc.cn

Liang Dong
CNLC International Kazakhstan Inc LLP, Almaty, Kazakhstan
liangdong@cnlc.cn

Kazim Nadirov
M. Auezov South Kazakhstan University, Shymkent, Kazakhstan
nadirovkazim@mail.ru

Ardak Yskak
Satbayev University, Kazakhstan
yskakardak@gmail.com (corresponding author)

Manap Zhantasov
M. Auezov South Kazakhstan University, Shymkent, Kazakhstan
manapjan_80@mail.ru

Saltanat Baibotayeva
M. Auezov South Kazakhstan University, Shymkent, Kazakhstan
sbaibotaeva@mail.ru

Received: 4 December 2025 | Revised: 12 January 2026 and 7 February 2026 | Accepted: 8 February 2026

 DOI: https://doi.org/10.48084/etasr.16703

ABSTRACT

Oil recovery from carbonate reservoirs is often limited by their heterogeneous permeability and complex fracture networks. This study investigates high-pressure gas injection as a method of enhancing oil displacement and maintaining reservoir pressure. Laboratory experiments were conducted on oil-saturated carbonate cores and sand-packed analogs to simulate flow redistribution and near-wellbore pressure conditions. The results indicate that maintaining elevated pressure within the elastic deformation range of rock and fluids promotes uniform lateral and vertical displacement, reduces preferential flow through high-permeability zones, and mobilizes oil from small pores and capillaries. Nitrogen injection achieved 62–68% oil recovery, with efficiency increasing with pressure and exposure time. The recommended methods for improving gas distribution in heterogeneous reservoirs are the pre-injection of proppant into the near-wellbore zone and well water shutoff via perforation and injection of gel-forming nanofluids and microcement. The findings demonstrate the potential of high-pressure gas injection to enhance sweep efficiency, reduce water and gas breakthrough, and support effective reservoir management.

Keywords-oil recovery; carbonate reservoir; well; gas injection; matrix; recovery efficiency; Enhanced Oil Recovery (EOR)

I. INTRODUCTION

The development of oil reservoirs through pressure maintenance by injecting water (including polymer and surfactant solutions) or gases is a well-established approach of enhancing the recovery of geological oil reserves. However, in productive formations containing clay-rich materials that swell upon contact with fresh water, water injection for pressure support is generally ineffective. Therefore, both hydrocarbon gases (e.g., methane) and non-hydrocarbon gases, including carbon dioxide (CO_2), nitrogen, and flue gases, are widely applied in pressure maintenance systems [1]. Previous studies have indicated that CO_2 injection is a promising candidate for enhancing oil recovery in carbonate reservoirs. Moreover, miscible CO_2 injection demonstrates higher recovery efficiency compared to immiscible CO_2 injection in carbonate formations [2]. Relatively low oil recovery from reservoirs remains a critical challenge [3], with estimates suggesting that more than half of the oil remains unrecovered after primary and secondary production. This motivates the application of CO_2 injection for Enhanced Oil Recovery (EOR). Additionally, CO_2 injection contributes to the mitigation of greenhouse gas emissions. Experimental results have shown that substantial improvement in oil recovery can be achieved by injecting nitrogen followed by low-salinity water flooding, reaching recovery factors of approximately 24% of the residual oil [4]. The increase in greenhouse gas emissions has become a global concern [5]. CO_2, the primary greenhouse gas, accounts for approximately 64% of the enhanced greenhouse effect, exceeding the impact of other greenhouse gases. Considering the availability of suitable geological storage sites, the application CO_2 capture, underground storage, and EOR represents a practical approach of dealing with greenhouse gases. Primary oil recovery methods typically extract only 18–20% of the original oil in place [6]. EOR techniques allow the recovery of 30–60% of the original oil in place [7].

Among the most effective CO_2-based strategies is the Water-Alternating-Gas (WAG) injection [8]. In [8], the authors demonstrate that low-salinity water injection can increase oil production by approximately 10% compared to high-salinity water under similar reservoir conditions. Experimental core displacement studies [9] investigated WAG injection and identified that the optimal water-to-gas ratio ranges from 1:1.5 to 2:1 for EOR. The influence of oil saturation, well placement, reservoir heterogeneity, and permeability anisotropy on the efficiency of water and CO_2 injection was quantitatively evaluated in [10]. Alternative injection schemes, such as simultaneous water and gas injection, were proposed in [11] to improve both recovery efficiency and economic performance, while also highlighting the risk of early CO_2 breakthrough at low water-to-CO_2 ratios. Carbonated water injection is particularly applicable in reservoirs where conventional waterflooding leaves significant residual oil. It was experimentally investigated in [12], demonstrating that increasing the volume of active carbonated water can enhance oil recovery, reaching a maximum recovery factor of 64%. The effectiveness of this method is attributed to the higher solubility of CO_2 in water and its lower miscibility pressure compared to other gases [13]. Related mechanisms were analyzed in [14]. The impact of rock heterogeneity on cyclic gas injection efficiency was highlighted in [15], where numerical modeling of cyclic CO_2 injection in the Bakken formation showed an incremental recovery of 9.17% over primary depletion. Cyclic CO_2 injection is widely studied due to its ability to enhance productivity in low-permeability reservoirs and its potential contribution to CO_2 sequestration [16]. Detailed experimental investigations of CO_2 miscible flooding, including dominant EOR mechanisms and the effects of adjuvants under varying pressure conditions, were conducted using core displacement and NMR imaging experiments in [17]. The effect of various CO_2 injection volumes on the gas–water contact, water-drive activity, and the waterflooding performance of producing wells to optimize the development of reservoirs characterized by elastic water-drive mechanisms was investigated in [18]. Simulation results indicate that increasing CO_2 injection volume enhances cumulative gas production while significantly reducing water production, with the main effect achieved at injection rates of up to 300,000 m³/day.

Co-injection of steam and gas has been demonstrated to increase oil recovery in heavy oil reservoirs [19], with potential production gains that reach 40% due to mechanisms such as gas displacement, oil swelling, and steam isolation. Laboratory studies have confirmed the advantage of sequential water and CO_2 injection in improving oil recovery [20]. Moreover, CO_2 injection has been evaluated for enhanced natural gas recovery and storage in depleted conventional and unconventional reservoirs, demonstrating ecological and economic feasibility [21]. Supercritical CO_2 flooding can achieve higher oil recovery in shale reservoirs [22], with average recovery factors of 46.98% at low and 73.35% at high displacement pressures. Core permeability after CO_2 flooding ranges from 28% to 64% of the initial values. Multicomponent gas injection is more effective than single-component injection [23]. For instance, CH_4 reduces the viscosity and density of light oil, while CO_2 decreases viscosity but increases density. Numerical simulations indicate that CO_2 extracts more heavy components into the vapor phase, whereas CH_4 favors the extraction of light components during cyclic gas injection. [24]. CO_2 injection also addresses two major challenges in shale reservoirs: reducing carbon emissions and enhancing unconventional oil recovery [25], as supported by experimental and modeling studies. The adsorption capacity of CO_2 in Eagle Ford (EF) shale was investigated under varying temperatures using six isothermal adsorption models [26]. Volumetric adsorption experiments conducted at pressures up to 12 MPa and temperatures of 35°C, 55°C, and 70°C showed that adsorption capacity increases with pressure and decreases with temperature, consistent with the exothermic nature of CO_2 adsorption.

Multiple factors influence CO_2 injection efficiency, with near-miscible or immiscible conditions significantly affecting displacement outcomes [27]. CO_2-based EOR has emerged as the dominant gas injection method in both mature and waterflooded carbonate reservoirs. Geological storage in oil and gas fields and saline aquifers represents a promising long-term solution, and high-resolution 3D geological frameworks integrating structural, lithological, and petrophysical data have identified structurally isolated zones suitable for CO_2 storage [28], characterized by minimal faulting, adequate reservoir thickness, high porosity, and high water saturation.

Technological advancements, including real-time reservoir simulation, 4D seismic monitoring, smart well technologies, and machine learning integration, have been critical for optimizing gas injection and reservoir management [29]. CO_2 injection has the benefit of enhancing oil recovery while reducing CO_2 emissions [30]. Modeling studies show that bottom-hole pressure has minimal impact on oil production, whereas increased injection rates can raise cumulative oil recovery by 33.39% and extend reservoir life from 20 to 37 years. Authors in [31] provide a novel comparative analysis of the SS and CA technologies applied to Indonesian natural gas fields, using Aspen HYSYS simulations and economic modeling to deliver practical, scalable insights for optimizing CO_2 capture strategies.

Overall, the effect of gas-based enhanced oil recovery methods is governed by several mechanisms: oil swelling due to gas dissolution, oil viscosity reduction, oil miscibility, residual oil mobilization, and viscosity equalization at the displacement front during oil–gas mixing. However, practical experience indicates that these reservoir pressure maintenance techniques, when applied in formations with heterogeneous pore permeability and fracture networks, are insufficient to achieve oil recovery factors exceeding 40–45% [30-31]. This limitation is primarily due to the insufficient understanding of the factors controlling oil displacement over the full extent and profile of the reservoir.

II. ANALYSIS OF RESERVOIR PRESSURE MAINTENANCE IN CARBONATE FORMATIONS THROUGH GAS INJECTION

Practical experience demonstrates that during reservoir pressure maintenance in carbonate formations through gas injection, premature gas breakthrough often occurs along large fractures and high-permeability zones across the reservoir area (Figure 1(a)) and vertically through the profile (Figure 1(b)), reaching the production wells. A significant volume of immobile oil remains beyond the advancing gas front, while the wellbore receives an intensive inflow of gas.

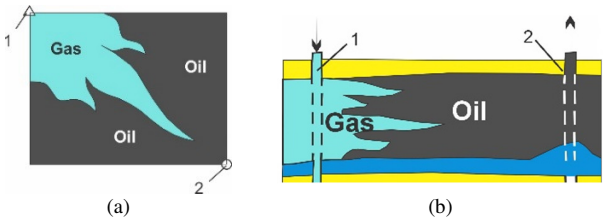

(a) (b)

Fig. 1. Gas breakthrough along paths of least resistance and through high-permeability zones of the reservoir: (a) across the areal extent, (b) across the vertical profile, into production wells.

This can be explained by the fact that reservoir pressure plays a dominant role during oil displacement over the full extent and profile of a reservoir. Lower reservoir pressure results in reduced elastic deformation of both the rock and the fluids, decreasing the likelihood of uniform oil displacement by the gas. Under such conditions, the gas tends to migrate along the paths of least resistance, leading to early breakthrough in production wells that intercept only a limited portion of the oil.

The existing configuration of compressor stations at injection wells and pump units at low-production wells does not allow achieving high reservoir pressure within the elastic energy range of the rock, gas, and oil system, due to the fact that the compressor at the injection well side generates a total pressure p_1, which consists of the pressure required to overcome gas flow resistance in the reservoir p_{11}, the negative pressure of the gas column inside the tubing p_{12}, and the pressure needed to overcome oil filtration resistance in the formation p_{13}. On the production well side, the pump generates a total pressure p_2 which includes the pressure required to overcome the resistance to the oil flow within the tubing p_{21} and the pressure exerted by the oil column inside the production well tubing p_{22}:

$$p_1 = p_{11} + p_{12} + p_{13} = \frac{\lambda}{2d} H v_1^2 g - \rho_1 g H + vL\mu \frac{\mu}{k} \quad (1)$$

$$p_2 = p_{21} + p_{22} = \rho_2 g H + \frac{\lambda}{2d} H v_2^2 \quad (2)$$

where ρ_1 and ρ_2 are the densities of gas and oil, respectively, H is the reservoir depth, λ is the friction factor for gas or oil flow inside the tubing, v_1 and v_2 are the flow velocities of gas and oil, respectively, g is the acceleration due to gravity, d is the tubing diameter, L is the drainage radius, μ is the oil viscosity, and k is the reservoir permeability.

The pressure distribution diagram (Figure 2(a)) demonstrates that the reservoir pressure generated is very low, and its magnitude is always below the threshold of elastic deformation of the rock matrix and fluids, and below the oil saturation pressure. The downhole pump on the production well side creates a vacuum in the near-wellbore zone, reducing the reservoir pressure established by the compressor on the injection well side.

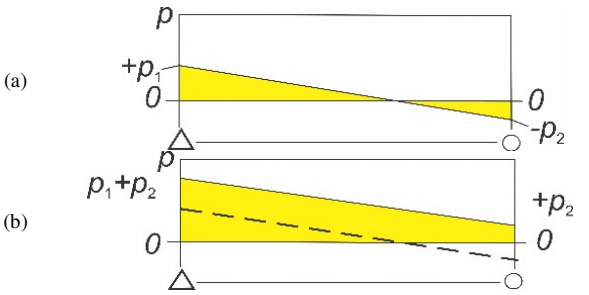

Fig. 2. Pressure distribution in the reservoir under the (a) existing and (b) the proposed configurations of compressor and pump installations for injection and production wells.

Under such low-pressure conditions, gas displaces oil from the reservoir over a limited area with poor sweep efficiency, moving preferentially along the path of least resistance and eventually breaking through into the production well. As a result, a significant volume of unrecovered oil remains on both sides of the gas flow within the reservoir. Therefore, the mechanism of gas breakthrough through the oil stream into production wells across the areal and vertical profiles of the reservoir follows the pattern illustrated in Figure 1.

One of the factors significantly contributing to low oil recovery in reservoirs is the presence of residual oil within the

pore space of fractured carbonate rock matrices. It should be noted that during the process of oil displacement by gas, inflow to the wellbore primarily occurs from fractures and cavities located between the carbonate rock matrices (Figure 3(a)). Oil contained within the small pores of each matrix is retained by capillary forces and surface tension, and under conventional conditions, a significant portion of this oil remains unrecovered from the reservoir.

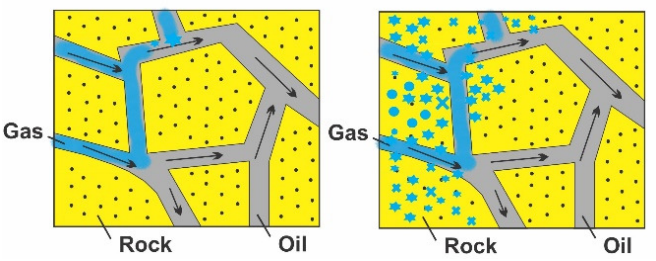

Fig. 3. Oil displacement from fractures and pore spaces of carbonate rock matrices under (a) low and (b) high reservoir pressure.

Injecting nitrogen under high pressure into the near-wellbore zone of a formation allows a significant portion of the oil to be extracted from the internal voids of the rock matrix and be directed to the bottomhole of a production well (Figure 3(b)). This is because nitrogen, a gas with a low density compared to oil, under high pressure begins to rapidly penetrate the small pores and capillaries of the matrix, displacing oil into cracks and caverns.

At present, the issue of water influx into the wellbore from aquifers through the annular space of wells remains unresolved. The existing water shutoff technology, which involves injecting gel-forming agents into the water-swept portion of the oil reservoir, does not effectively reduce the water cut of produced oil. Thus, under the current system of reservoir pressure maintenance by gas injection, complete oil displacement across the areal and vertical profiles of the reservoir, as well as from the pore spaces of fractured carbonate rock matrices, is not achieved. Further improvement of water shutoff technologies for production wells is therefore required.

III. METHODOLOGY OF HIGH-PRESSURE GAS INJECTION IN CARBONATE RESERVOIRS

The proposed method of enhancing oil recovery by creating high reservoir pressure exceeding the oil saturation pressure with gas is protected by two issued patents, No. 36487 RK (Bulletin No. 48, 01.12.2023) and No. 37002 RK (Bulletin No. 43, 24.10.2024). The method consists of generating elevated reservoir pressure during gas injection into the oil reservoir using an injection well compressor. The pressure is established within the range of high elastic deformation of the rock and fluids, exceeding both the oil filtration pressure through the rock pores and the lifting pressure required for oil production to the surface through production wells. In this configuration, a centrifugal pump is installed at the wellhead of the production well to transport oil to the gathering facility.

The total reservoir pressure p developed by the compressor on the injection well side can be expressed as the sum of the pressures required to overcome: the flow resistance of water inside the tubing, the gravitational force of the gas column within the injection well (with a negative sign), the oil filtration resistance in the reservoir, and the flow resistance of oil inside the tubing along with the gravitational force of the oil column in the production well:

$$p = \frac{\lambda}{2d} H v_1^2 g - \rho_1 g H + vL\mu \frac{\mu}{k} + \rho_2 g H + \frac{\lambda}{2d} H v_2^2 \quad (3)$$

From (3) and the pressure distribution changes (Figure 2(b)), it is evident that installing a compressor on the injection well side without a downhole pump in the production well significantly increases the reservoir pressure without changing the overall power consumption of the pressure maintenance system. Under uniform compression, the strength limits of the rock are much higher than under standard atmospheric conditions. For reservoirs with maximum depths of up to 5000 m, the in-situ stress is below 100 MPa, which is significantly lower than the elastic limit of 150–160 MPa. This indicates the feasibility of generating high reservoir pressure within the elastic range of the rock and fluids.

The pressure distribution in the reservoir between the injection and production wells with a compressor installed at the injection well is shown in Figure 2(b). Oil displacement across the reservoir area and profile (Figure 4) can be achieved by creating high reservoir pressure within the elastic deformation range of the rock, exceeding both the oil saturation pressure with the gas and the filtration resistance in the formation. This is explained by the fact that under high reservoir pressure, the elastic compressive forces facilitate more uniform oil displacement toward the production wells.

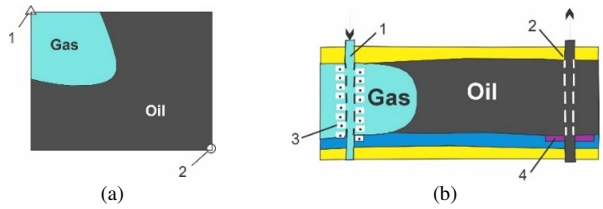

Fig. 4. (a) Oil displacement across the reservoir area and (b) profile under high reservoir pressure: 1 and 2 – injection and production wells, respectively; 3 – coarse-grained sand or proppant layer; 4 – water-shutoff screen.

From the perspective of material balance between the injected gas and the produced oil, it is more appropriate to maintain a ratio of production wells to injection wells equal to or close to 1. For example, five-, seven-, and nine-spot well patterns can be considered effective, with a production well located at the center and injection and production wells arranged alternately along the edges.

By the end of field development, the residual oil in the reservoir can be recovered by converting the central production well into an injection well. Such well-pattern configurations, combined with the creation of high reservoir pressure within the elastic deformation range of the rock, promote uniform oil displacement by water over a large area without water breakthrough through the oil flow into the production wells. To ensure uniform delivery of the injected gas into the near-

wellbore zone of the injection well (1) (Figure 4) along the reservoir height and effective displacement of oil toward the production well (2), a layer of coarse sand or proppant (3) is injected into the near-wellbore zone of the oil reservoir through perforated channels of the production casing. This promotes uniform oil displacement by the gas throughout the height of the carbonate reservoir, even in formations with heterogeneous fracturing and permeability. The new water shutoff technology involves creating impermeable screens (4) below and above the oil-bearing zone by perforating the production casing and injecting a gel-forming nanofluid $Na_2O(SiO_2)_n$ with a stabilizer into the reservoir using mineralized formation water, while the annular channels are filled with a microcement-based expanding grout.

Various mechanical and physicochemical methods have been studied to enhance reservoir performance and reduce water cut by selectively affecting fluid flow within the formation. Implosion-based stimulation techniques, such as those described in [32], demonstrate the potential to restore permeability and improve well productivity by removing the drilling-induced colmatation in aquifers. While polymer gels remain widely used for water shutoff, their interaction with oil-saturated zones often leads to undesirable permeability reduction and oil production loss, particularly in radial flow conditions [33]. These findings emphasize the need for alternative approaches, such as controlled reservoir pressure manipulation, to improve sweep efficiency without impairing oil mobility.

The success of pressure-based water cut reduction methods largely depends on the accuracy of reservoir diagnostics. Authors in [34] demonstrated that integrating electrical inverse lateral logging with radioactive methods significantly improves the reliability of formation property assessment in cased wells, enabling better-informed decisions for reservoir stimulation planning. Authors in [35] developed a cost-effective gel-based water shutoff agent for the Kalamkas field, highlighting the importance of tailored formulations for profile leveling and reduction of water inflow.

Injection of nitrogen at high pressure into the near-wellbore zone of the reservoir allows a significant portion of the oil to be recovered from the pores and capillaries of the carbonate rock matrices and directed toward the production wellbore (see Figure 3(a)), due to the fact that gas, having a lower density than oil, under high pressure penetrates the small pores and capillaries of the matrix and displaces oil into fractures and cavities. This process can be mathematically described based on the force balance acting on the oil particles within the small pores and capillaries of the matrix:

$$mg + p_0 s_0 - F_{fr} - F_A = 0 \quad (4)$$

where mg is the gravitational force of the oil particles, $p_o\, s_o$ is the gas pressure force acting on the unit area of the pores and channels of the carbonate rock matrix, F_A is the buoyant force, and F_{fr} is the frictional force of the oil particles against the rock surface. The frictional force acting on an oil element in contact with the pore wall can be expressed, according to Newton's law of viscosity, as:

$$F_{fr} = -\mu S \frac{dv}{dr} \quad (5)$$

where μ is the dynamic viscosity of the oil, $S = 2\pi r_o l$ is the surface area of the pore or capillary wall, and r_o and l are the pore radius and length, respectively.

For viscous flow of a Newtonian fluid in pore-scale capillaries, a parabolic velocity distribution consistent with Poiseuille flow is assumed:

$$\upsilon(r) = \upsilon_{max}\left(1 - \frac{r^2}{r_0^2}\right) \quad (6)$$

where υ_{max} is the maximum velocity at the center of the pore. Differentiating with respect to the radial coordinate r, the velocity gradient is given by:

$$\frac{d\upsilon}{dr} = -\frac{2\upsilon_{max} r}{r_0^2}$$

At the pore wall ($r=r_0$), the velocity gradient becomes:

$$\left.\frac{d\upsilon}{dr}\right|_{r=r_0} = -\frac{2\upsilon_{max}}{r_0}$$

Substituting the expressions for the surface area S and the velocity gradient into (5), the frictional force acting along the pore wall can be written as:

$$F_{fr} = -\mu(2\pi r_0 l)\left(-\frac{2\upsilon_{max}}{r_0}\right) = 4\pi\mu l \upsilon_{max} \quad (7)$$

It should be noted that pore-scale oil displacement cannot be explained solely by the density differences between phases. In low-permeability and microporous media, the movement of the fluids is primarily governed by capillary pressure, interfacial tension, wettability, and relative permeability. In particular, gas penetration into micropores occurs only when the applied pressure gradient exceeds the capillary entry pressure, which depends on pore radius, interfacial tension, and contact angle. Therefore, viscous forces act in conjunction with capillary forces, and their combined effect controls fluid displacement at the pore scale. The body force acting on the oil phase due to gravity can be expressed as:

$$F_g = \rho_a V g = \pi r_0^2 l \rho_o g \quad (8)$$

while the contribution associated with the gas phase occupying the pore volume is given by:

$$F_a = \rho_a V g = \pi r_0^2 l \rho_a g \quad (9)$$

The balance of forces acting along the pore axis, including the pressure force, viscous resistance, and gravity-related body forces, can be written as:

$$p_0 s_0 - 4\pi\mu l \upsilon_0 - \pi r_0^2 l(\rho_o - \rho_a)g - p_c s_0 = 0 \quad (10)$$

where p_c is the capillary entry pressure required for the gas to invade the oil-filled pores.

Solving (10) with respect to the applied pressure yields:

$$p_0 = \frac{4\pi\mu l \upsilon_0 + \pi r_0^2 l(\rho_o - \rho_a)g}{s_0} + p_c \quad (11)$$

This expression demonstrates that the gas-driven oil displacement at the pore scale is governed by the combined effect of viscous forces, gravity-related density contrast, and capillary resistance. In microporous and low-permeability

media, capillary pressure represents the dominant resistance to gas entry, while density differences play a secondary role.

As gas propagates through fractures and cavities, it first occupies the largest flow paths and subsequently invades smaller pores only when the applied pressure exceeds the capillary entry pressure. The maintenance of elevated reservoir pressure within the elastic deformation range of the rock promotes more uniform gas sweep and enhances oil mobilization without premature gas or water breakthrough. From a field-scale perspective, balanced injection–production strategies are required to sustain pressure and ensure efficient displacement. Well patterns with approximately equal numbers of injection and production wells (e.g., five-, seven-, or nine-spot patterns) provide favorable pressure support and sweep efficiency. At the late stage of field development, the conversion of central production wells into injection wells can further improve the recovery by maintaining the reservoir pressure and enhancing the gas-assisted oil displacement.

IV. EXPERIMENTAL METHODOLOGY

The experiment aimed to justify the feasibility of high reservoir energy generation, ensuring uniform oil displacement across the reservoir area and profile while preventing gas breakthrough into production wells. Initially, gas filtration processes through models of porous clastic formations were studied on the laboratory setup (Figure 5) under the influence of both inelastic and elastic forces. The laboratory setup represents a reservoir model and consists of one horizontal (1) and two vertical cylindrical working chambers (2-3), which are filled with rock samples – quartz sand with particle sizes of 0.6–0.8 mm. The working chambers are sequentially connected to each other via flexible pipelines (4) and (5). The horizontal working chamber is equipped with a nozzle (6) with a manometer and a valve for water supply, and another nozzle (7) with a manometer and a valve for gas (air) supply from a compressor (8), which also has a manometer and a valve. The vertical working chambers are equipped with an inlet nozzle (9) at the bottom and an outlet nozzle (10) at the top, both with manometers and valves, as well as valves (11) for water drainage. Receiving tanks (12) are located under the outlet nozzles (10). The working chambers, compressor, and receiving tanks are mounted on the frame (13). The main dimensions of the working chambers are: internal pipe diameter = 80 mm, length = 550 mm. The rock material (sand (14) inside the working chambers is confined between the thin layers (15) of solid granular materials with variable particle sizes of 1.0–2.0 mm and a circular plate mesh (16) with hole diameters of 1.5 mm. This configuration allows the sand sample to maintain a consistent water filtration rate.

In the pores of the horizontal working chamber, an inelastic force is generated by injecting water, while an elastic force is created by injecting gas (air). Initially, the process of oil displacement by water was studied under conditions without creating an elastic medium in the rock pores. Water at a pressure of 0.65 MPa is supplied through the inlet nozzle 6 into the horizontal working chamber (1). The water is divided into two streams, left and right. The left water stream passes through the pores of the rock sample in the horizontal chamber (1) and the left vertical chamber (2), and then enters the left receiving tank (12) via the outlet nozzle (10). The right water stream passes through pipeline (4) and the pores of the rock sample in the right vertical working chamber (3), and then enters the right receiving tank (12) via the outlet nozzle (10). The volume of the water collected in the tanks is measured at specified time intervals.

(a)

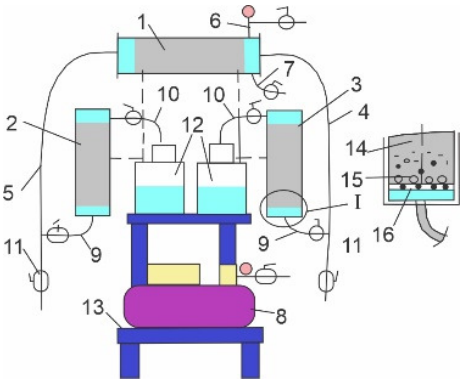

(b)

Fig. 5. (a) Schematic (a) and (b) overall view of the laboratory experimental setup: 1 – horizontal working chamber; 2, 3 – vertical working chambers; 4, 5 – pipelines; 6, 7 – nozzles; 8 - compressor; 9 – inlet nozzle, 10 – outlet nozzle; 11 – valve; 12 – tank; 13 – frame; 14 – rock material – sand; 15 – thin layers of solid granular materials; 16 – circular plate mesh.

It should be noted that the incoming water flows from the inlet nozzle (6) in two directions with different filtration resistances. The right stream experiences lower filtration resistance than the left stream, as it passes only through the rock of the right vertical working chamber (3). Therefore, in the experimental setup, the right water stream models the flow of the water in the reservoir toward the production wells along the path of least resistance, i.e., the shortest path between the injection and production wells. The left stream, in contrast, encounters higher filtration resistance because it passes through the rocks of two working chambers, horizontal (1) and vertical (2). In the setup, the left water stream simulates the displacement of oil in an inelastic reservoir toward production wells at the edges of the water-oil displacement front. Consequently, the volume of the water collected per time unit in the left receiving tank is lower than that in the right receiving tank due to the large difference in the filtration resistances experienced by the left and right streams through the rock pores. This behavior was confirmed by the conducted experiments.

V. RESULTS AND DISCUSSION

The measurement results of water entry time t (s) and volumes V_1 and V_2 (10^{-3} m³) into the receiving tanks under pressure p (MPa), as well as the calculations of water flow rates Q_1 and Q_2 (10^{-6} m³/s) during the conducted experiments without creating an elastic medium in the rock pores, are presented in Table I and Figure 6. All experiments were conducted in triplicate to ensure reproducibility, and the results reported are the mean values. Measurement uncertainties were estimated using standard statistical methods, including calculation of standard deviations. The pressure in the working chambers was monitored and allowed to stabilize before recording data, ensuring that the measurements reflected the steady-state conditions. All pressures and flow rates were measured using calibrated instruments and standard data acquisition systems. From Table I and Figure 6, it is evident that as the filtration resistance of the water in the rock increases, the transported volume V_1 significantly decreases, whereas a reduction in filtration resistance leads to an increase in the transported volume V_2. This indicates that in a reservoir, a substantial portion of the water would flow along the path of least resistance, while a smaller portion would move along the flanks. Under real field conditions, this would result in premature water breakthrough in the production wells. Premature water influx is further exacerbated by the creation of a vacuum in the reservoir by plunger pumps of the production wells.

TABLE I. EXPERIMENTAL RESULTS WITHOUT ELASTIC MEDIUM FORMATION IN ROCK PORES

№	t (s)	p (MPa)	V_1 (10^{-3} m³)	V_2 (10^{-3} m³)	Q_1 (10^{-6} m³/sec)	Q_2 (10^{-6} m³/sec)
1	60	0.65	3.0	5.1	50.0	85.0
2	90	0.65	4.5	7.7	50.0	85.5
3	120	0.65	5.9	10.2	49.2	85.0

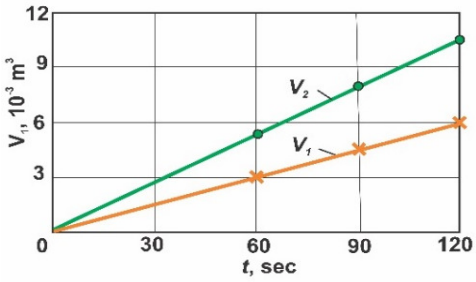

Fig. 6. Dependence of the volumes of the left (V_1) and right (V_2) water streams passing through the rock samples of the working chambers on time t.

Moving on, the patterns of the oil displacement from the reservoir by the gas were studied under the creation of an elastic force in the rock pores. For this purpose, the two vertical working chambers (2) and (3) in Figure 5 were filled with water, and the valves of the inlet nozzle (6) of the horizontal working chamber and the inlet valve (9) of the vertical working chamber were closed. Water was then drained from the horizontal working chamber through the valves of nozzles (11) and (7). The outlet valve (10) was opened. A flexible pipeline from the compressor (8) was connected to the nozzle (7) of the horizontal working chamber. The compressor motor was switched on. Gas (air) from the compressor cylinder at a pressure of 0.60 MPa flowed through nozzle (7) into the pores of the rock in the horizontal working chamber (1), and then, through pipelines (4) and (5), began displacing water from the pores of the rock in the two vertical working chambers (2) and (3). The displaced water, passing through the two outlet nozzles (10,) entered the receiving tanks (12). The time of water outflow and the volume collected in the receiving tanks were measured. The experiment was repeated at a higher pressure in the compressor cylinder, and each measurement under elastic medium conditions was conducted three times. The results are presented in Table II and Figure 7.

TABLE II. EXPERIMENTAL RESULTS UNDER ELASTIC FORCE CONDITIONS IN ROCK PORES

№	t (s)	p (MPa)	V_1 (10^{-3} m³)	V_2 (10^{-3} m³)	Q_1 (10^{-6} m³/sec)	Q_2 (10^{-6} m³/sec)
1	120	0.60	6.0	6.0	50.0	50.0
2	100	0.80	6.0	6.0	60.0	60.5
3	80	1.00	6.0	6.0	75.0	75.0

It should be noted that filling the pores of the rock in the horizontal working chamber with compressible gas (air) under pressure simulates the process of creating high pressure in the reservoir within the elastic deformation region of the rock and fluids, thereby enabling more complete oil displacement from the reservoir by water. From Table II and Figure 7, it is evident that during the creation of an elastic medium in the horizontal working chamber by gas injection under pressure, the water volumes that pass through the left and right vertical working chambers are equal.

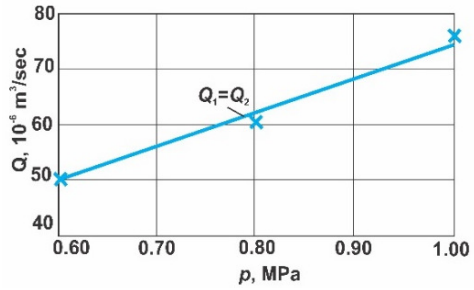

Fig. 7. Dependence of the water flow rates ($Q_1 = Q_2 = Q$) for each working chamber on the pressure (p) generated by the compressor.

This demonstrates the advantage of creating an elastic high pressure in the reservoir, which allows for uniform displacement of the oil by the water throughout the reservoir. These procedures, including repeated measurements, monitoring of pressure stabilization, and statistical estimation of measurement errors, provide confidence in the reliability and reproducibility of the experimental results. Laboratory studies were also conducted to identify the main mechanism of residual oil displacement from the matrices of fractured-porous carbonate rock by nitrogen, and to experimentally determine the optimal regimes and parameters for nitrogen injection technology in multilayer oil reservoirs [36]. The experimental results showed that the proportion of oil displaced from oil-saturated carbonate core samples ranged from 62% to 68%, and the efficiency of displacement significantly depended on the exposure duration (volume of injected nitrogen) and pressure. Nitrogen, under high pressure, begins to penetrate intensively into the small pores and

capillaries of the matrix, displacing oil into fractures and cavities.

Theoretical considerations and laboratory experiments demonstrated the possibility of significantly increasing oil recovery and reducing water production from wells by creating elastic high reservoir pressure within the elastic deformation region of the rock and fluids, exceeding the filtration pressure of the oil through the rock pores and the pressure required to lift oil to the surface through production wells, but not lower than the oil saturation pressure by hydrocarbon gases. In this case, the production wells are not equipped with pumps, and as water breakthrough occurs, the producing wells are converted into injection wells.

VI. METHODOLOGY OF HIGH-PRESSURE GAS INJECTION EXPERIMENTS IN CARBONATE CORE SAMPLES

To investigate the oil displacement from carbonate reservoirs using high-pressure gas injection, laboratory experiments were conducted on real limestone core samples in collaboration with specialists from PetroQazaqstan, Kazakhstan. A total of five experiments were carried out, with three repetitions for each experimental condition to ensure reproducibility. The cores were saturated with crude oil from the Karabulak field (density 0.735 g/cm³, viscosity 1.34 mPa·s) to simulate reservoir conditions. The general appearance of the oil-saturated limestone core samples used in the experiments is shown in Figure 8.

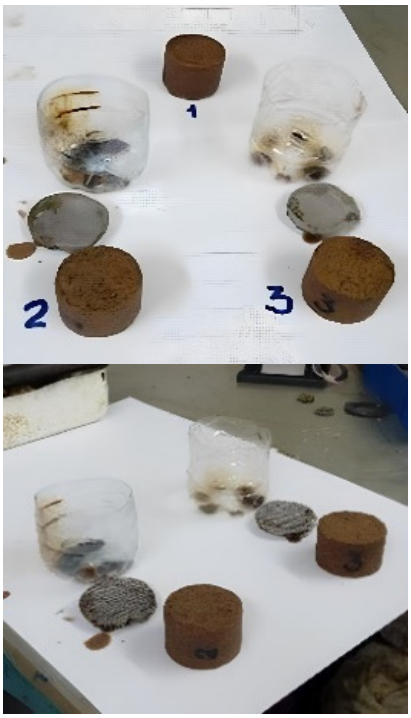

Fig. 8. Oil-saturated limestone core samples used in the high-pressure gas injection experiments.

Experiments were conducted on two laboratory setups. The first setup was designed to study the mechanism of oil displacement from the pore space of carbonate core samples by high-pressure nitrogen (Figure 9). The second setup was used to determine the extent of oil displacement from carbonate core samples by nitrogen under uniaxial loading conditions (Figure 10). The first laboratory setup (Figure 9) consisted of a horizontal cylindrical housing (1) with an end cap (2). The cylindrical housing had a diameter of 127 mm and a length of 400 mm. The cap was attached to the housing with a flanged connection and bolts through a paronite gasket, which ensured the sealing of the working chamber. Two pipes, (3) and (4), were attached to the top of the cylindrical housing, and were used to attach a pressure gauge (5) and a reinforced rubber hose (6). A socket (7) was attached to the cover, with its blind end located inside the working chamber of the housing, and a thermometric sensor (8) is inserted into its open end. Core samples (9) were placed inside the working chambers in special cups (10). A free space at the bottom of the cups was created by a mesh partition. The working chamber was connected to a nitrogen cylinder (11) via a reinforced rubber-fabric hose through a reducer (12) with pressure gauges. The nitrogen inside the cylinder was under a pressure of 15 MPa. Electric heaters (13) were attached to the bottom of the cylindrical body to create a formation temperature inside the working chamber. A reserve chamber (14) was installed below the cylindrical body, having a connecting pipe (15) with a faucet (16). The reserve chamber was equipped with an outlet pipe (17) and a faucet (18). The cylindrical body and the reserve chamber were mounted on a frame (19). The temperature sensor was connected to a thermometer.

(a)

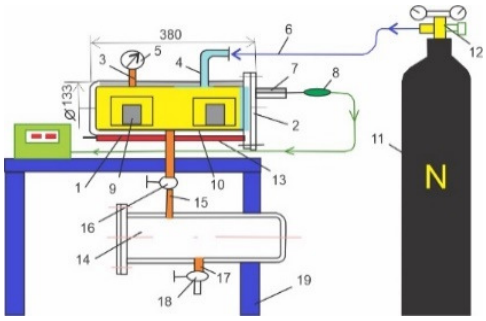

(b)

Fig. 9. (a) Schematic and (b) general view of the setup: 1 - horizontal cylindrical housing; 2 - end cap; 3, 4 - pipes; 5 - pressure gauge; 6 - reinforced rubber hose; 7 – socket; 8 - thermometric sensor; 9 – core; 10 - special cup; 11 - nitrogen cylinder; 12 – reducer; 13 - electric heaters; 14 - reserve chamber; 15 – pipe; 16 – faucet; 17 - outlet pipe; 18 – faucet; 19 – frame.

This configuration allowed controlled investigation of the nitrogen-driven oil displacement under high pressure and the assessment of the recovery efficiency and the flow redistribution mechanisms in the carbonate matrix.

Figure 10 shows the schematic and overall view of the second laboratory setup, which consisted of a horizontal cylindrical body (1) with a working chamber designed to accommodate a rubber gasket (2), a core sample (3), and a rubber seal (4). One end of the cylindrical body had an internal thread, allowing connection to the end pipe (5). An inlet pipe (6) was attached to one end of the cylinder via a flange connection. The pressure inside the working chamber of the cylinder was measured by the pressure gauge (7). The end pipe (5) of the cylinder was connected via a reinforced rubber hose (8) to the gas meter (9).

Each core was cleaned with pressurized air, weighed, and then saturated with oil in containers for 10–12 hours. To remove residual air bubbles, the saturated cores were placed in a vacuum chamber before the experiments. The initial core properties are presented in Table III.

(a)

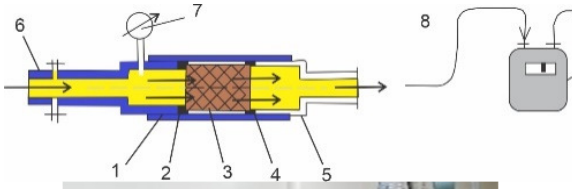

(b)

Fig. 10. (a) Schematic and (b) general view of the second setup 2: 1- horizontal cylindrical body; 2 - rubber gasket; 3 - core sample; 4 - rubber seal; 5 - end pipe; 6 - inlet pipe; 7 - pressure gauge; 8 - reinforced rubber hose; 9 - gas meter.

TABLE III. INITIAL CORE PROPERTIES

Core No.	Setup	Mass before oil saturation (g)	Mass after oil saturation (g)	Oil content (g)
1	Second	86.61	94.29	7.68
2	First	85.59	89.75	4.16
3	First	83.60	87.73	4.13
4	First	89.08	93.60	4.52
5	Second	77.87	84.89	11.11

The initial oil content of the cores ranged from 4.13 to 11.11 g. The results of nitrogen injection into the pores of carbonate cores are presented in Table IV. The experiments show that nitrogen injection displaced 62–68% of the oil from the cores. The displacement efficiency increased with higher pressure and longer injection time.

These results demonstrate that nitrogen injection can significantly enhance oil recovery, and the technique can be applied both in the near-wellbore zone of producing wells and via injection wells to maintain reservoir pressure.

TABLE IV. RESULTS OF NITROGEN INJECTION INTO THE PORES OF CARBONATE CORES

Core No.	Setup	Oil before N_2 injection (g)	Chamber pressure (bar)	Oil after N_2 injection (g)	Oil displacement (%)
1	Second	7.68	5	2.76	64
2	First	4.16	5	1.55	63
3	First	4.13	6	1.51	63
4	First	4.52	8	1.74	62
5	Second	11.11	8	2.61	68

VII. CONCLUSIONS

From the theoretical analysis and the laboratory experiments conducted on oil-saturated carbonate core samples, the following conclusions can be drawn:

- Oil recovery from reservoirs is often limited by heterogeneous permeability, complex rock structure, and low reservoir pressure. High-pressure gas injection has been investigated as a method for enhancing oil recovery and maintaining reservoir pressure.
- When high reservoir pressure is created, the matrix of a porous or fractured rock expands, while the oil and gas are highly compressed, accumulating enormous natural energy throughout the reservoir. This high reservoir energy is capable of uniformly displacing oil toward production wells. High reservoir energy can be maintained and controlled by choking wellhead equipment or by adjusting the pump capacity of the production well. The experiments conducted on a reservoir model confirm this assertion.
- Currently, the reservoir pressure at the oil fields is maintained within the range of 15–18 MPa, which is slightly higher than the saturation pressure of oil and gases (12–15 MPa). Modern compressor units, like pumping units, can create very high reservoir pressures, up to 60–80 MPa. This allows for an overall increase in oil production.
- The oil trapped in the small pores within each carbonate rock matrix is held by the capillary force and surface tension. Under normal conditions, a significant portion of the oil is not recovered from the reservoir. High-pressure nitrogen injection into the near-wellbore zone of the formation allows for the extraction of a significant portion of the oil from the internal voids of the rock matrix and its delivery to the bottomhole of the production well, because nitrogen, as a gas with a lower density than oil, under high pressure begins to rapidly penetrate the small pores and capillaries of the matrix, displacing oil from them into cracks and caverns. Experiments show that nitrogen injection displaced 62–68% of the oil from the cores.
- From the perspective of material balance between injected gas and produced oil, it is more appropriate to maintain a ratio of production to injection wells equal to or close to 1.

For example, five-, seven-, and nine-spot well patterns can be considered effective, with a production well located at the center and injection and production wells arranged alternately along the edges. By the end of field development, the residual oil in the reservoir can be recovered by converting the central production well into an injection well.

- To ensure the uniform delivery of the injected gas into the near-wellbore zone of the injection well along the reservoir height and the effective displacement of the oil toward the production well, a layer of coarse sand or proppant is injected into the near-wellbore zone of the oil reservoir through perforated channels of the production casing. This promotes uniform oil displacement by gas throughout the height of the carbonate reservoir, even in formations with heterogeneous fracturing and permeability.
- The new water shutoff technology involves creating impermeable screens below and above the oil-bearing zone by perforating the production casing and injecting a gel-forming nanofluid $Na_2O(SiO_2)_n$ with a stabilizer into the reservoir using mineralized formation water, while the annular channels are filled with a microcement-based expanding grout.

ACKNOWLEDGMENT

This research was funded by the Science Committee of the Ministry of Science and Higher Education of the Republic of Kazakhstan grant number BR24992809.

REFERENCES

[1] L. Lake, R. T. Johns, W. R. Rossen, and G. A. Pope, *Fundamentals of Enhanced Oil Recovery*. Society of Petroleum Engineers, 2014.

[2] H. Hawez and Z. Ahmed, "Enhanced Oil Recovery By CO_2 Injection In Carbonate Reservoirs," in *Energy and Sustainability V*, 2015, pp. 547–558.

[3] L. B. J. Chathurangani and B. M. Halvorsen, "Near Well Simulation of CO2 Injection for Enhanced Oil Recovery (EOR)," in *Proceedings of the 56th SIMS*, Linköping University, Sweden, Oct. 2015, pp. 309–318, https://doi.org/10.3384/ecp15119309.

[4] E. G. Lwisa and A. R. Abdulkhalek, "Enhanced oil recovery by nitrogen and carbon dioxideinjection followed by low salinity water flooding for tight carbonate reservoir: experimental approach," *IOP Conference Series: Materials Science and Engineering*, vol. 323, 2018, Art. no. 012009, https://doi.org/10.1088/1757-899X/323/1/012009.

[5] S. Ding, Y. Xi, H. Jiang, and G. Liu, "CO2 storage capacity estimation in oil reservoirs by solubility and mineral trapping," *Applied Geochemistry*, vol. 89, pp. 121–128, Feb. 2018, https://doi.org/10.1016/j.apgeochem.2017.12.002.

[6] O. Torsæter, "Application of Nanoparticles for Oil Recovery," *Nanomaterials*, vol. 11, no. 5, Apr. 2021, Art. no. 1063, https://doi.org/10.3390/nano11051063.

[7] A. Sircar, K. Rayavarapu, N. Bist, K. Yadav, and S. Singh, "Applications of nanoparticles in enhanced oil recovery," *Petroleum Research*, vol. 7, no. 1, pp. 77–90, Mar. 2022, https://doi.org/10.1016/j.ptlrs.2021.08.004.

[8] S. Naderi and M. Simjoo, "Numerical study of Low Salinity Water Alternating CO2 injection for enhancing oil recovery in a sandstone reservoir: Coupled geochemical and fluid flow modeling," *Journal of Petroleum Science and Engineering*, vol. 173, pp. 279–286, Feb. 2019, https://doi.org/10.1016/j.petrol.2018.10.009.

[9] S. Pancholi, G. S. Negi, J. R. Agarwal, A. Bera, and M. Shah, "Experimental and simulation studies for optimization of water–alternating-gas (CO2) flooding for enhanced oil recovery," *Petroleum Research*, vol. 5, no. 3, pp. 227–234, Sep. 2020, https://doi.org/10.1016/j.ptlrs.2020.04.004.

[10] B. Ren and I. J. Duncan, "Maximizing oil production from water alternating gas (CO2) injection into residual oil zones: The impact of oil saturation and heterogeneity," *Energy*, vol. 222, May 2021, Art. no. 119915, https://doi.org/10.1016/j.energy.2021.119915.

[11] S. M. M. Nasser, A. Bera, and V. Ramalingam, "Comparative studies on numerical sensitivity of different scenarios of enhanced oil recovery by water-alternating-gas (CO2) injection," *Petroleum Research*, vol. 8, no. 4, pp. 505–513, Dec. 2023, https://doi.org/10.1016/j.ptlrs.2023.07.001.

[12] X. Chen, A. Paprouschi, M. Elveny, D. Podoprigora, and G. Korobov, "A laboratory approach to enhance oil recovery factor in a low permeable reservoir by active carbonated water injection," *Energy Reports*, vol. 7, pp. 3149–3155, Nov. 2021, https://doi.org/10.1016/j.egyr.2021.05.043.

[13] A. Talebi, A. Hasan-Zadeh, Y. Kazemzadeh, and M. Riazi, "A review on the application of carbonated water injection for EOR purposes: Opportunities and challenges," *Journal of Petroleum Science and Engineering*, vol. 214, Jul. 2022, Art. no. 110481, https://doi.org/10.1016/j.petrol.2022.110481.

[14] Z. Sakhaei, M. Salehpour, and M. Riazi, "Carbonated water injection," in *Gas Injection Methods*, Gulf Professional Publishing, 2023, pp. 259–294.

[15] Y. Assef, A. Kantzas, and P. Pereira Almao, "Numerical modelling of cyclic CO2 injection in unconventional tight oil resources; trivial effects of heterogeneity and hysteresis in Bakken formation," *Fuel*, vol. 236, pp. 1512–1528, Jan. 2019, https://doi.org/10.1016/j.fuel.2018.09.046.

[16] J. Mugisha, S. Al-Rbeawi, and E. Artun, "Analytical modeling of flow regimes during cyclic CO2 injection in hydraulically fractured tight reservoirs for enhanced oil recovery," *Journal of Petroleum Science and Engineering*, vol. 201, Jun. 2021, Art. no. 108385, https://doi.org/10.1016/j.petrol.2021.108385.

[17] T. Wang, L. Wang, X. Meng, Y. Chen, W. Song, and C. Yuan, "Key parameters and dominant EOR mechanism of CO2 miscible flooding applied in low-permeability oil reservoirs," *Geoenergy Science and Engineering*, vol. 225, Jun. 2023, Art. no. 211724, https://doi.org/10.1016/j.geoen.2023.211724.

[18] S. Matkivskyi, O. Kondrat, and O. Burachok, "Investigation of the influence of the carbon dioxide (CO2) injection rate on the activity of the water pressure system during gas condensate fields development," *E3S Web of Conferences*, vol. 230, 2021, Art. no. 01011, https://doi.org/10.1051/e3sconf/202123001011.

[19] N. B. Zapata, J. M. M. Cárdenas, and J. J. M. Paternina, "Flue gas and nitrogen co-injection during cyclic steam stimulation in heavy oil reservoirs: a numerical evaluation," *DYNA*, vol. 88, no. 218, pp. 127–135, Aug. 2021, https://doi.org/10.15446/dyna.v88n218.90341.

[20] Q. Wang, J. Shen, P. Lorinczi, P. Glover, S. Yang, and H. Chen, "Oil production performance and reservoir damage distribution of miscible CO2 soaking-alternating-gas (CO2-SAG) flooding in low permeability heterogeneous sandstone reservoirs," *Journal of Petroleum Science and Engineering*, vol. 204, Sep. 2021, Art. no. 108741, https://doi.org/10.1016/j.petrol.2021.108741.

[21] A. Hamza, I. A. Hussein, M. J. Al-Marri, M. Mahmoud, R. Shawabkeh, and S. Aparicio, "CO2 enhanced gas recovery and sequestration in depleted gas reservoirs: A review," *Journal of Petroleum Science and Engineering*, vol. 196, Jan. 2021, Art. no. 107685, https://doi.org/10.1016/j.petrol.2020.107685.

[22] H.-B. Li *et al.*, "Mechanism of CO2 enhanced oil recovery in shale reservoirs," *Petroleum Science*, vol. 18, no. 6, pp. 1788–1796, Dec. 2021, https://doi.org/10.1016/j.petsci.2021.09.040.

[23] Z.-H. Jia *et al.*, "Effects of CH4/CO2 multi-component gas on components and properties of tight oil during CO2 utilization and storage: Physical experiment and composition numerical simulation," *Petroleum Science*, vol. 20, no. 6, pp. 3478–3487, Dec. 2023, https://doi.org/10.1016/j.petsci.2023.06.002.

[24] S. Du, S. Salasakar, and G. Thakur, "A Comprehensive Summary of the Application of Machine Learning Techniques for CO_2-Enhanced Oil Recovery Projects," *Machine Learning and Knowledge Extraction*, vol. 6, no. 2, pp. 917–943, 2024, https://doi.org/10.3390/make6020043.

[25] S. Qin, J. Li, J. Chen, X. Bi, and H. Xiang, "Research on Displacement Efficiency by Injecting CO2 in Shale Reservoirs Based on a Genetic Neural Network Model," *Energies*, vol. 16, no. 12, Jun. 2023, Art. no. 4812, https://doi.org/10.3390/en16124812.

[26] Z. H. Zardari and D. F. Mohshim, "Temperature Dependence Evaluation of CO2 Adsorption on Eagle Ford Shale using Isothermal Models: A Comparative Study," *Engineering, Technology & Applied Science Research*, vol. 15, no. 1, pp. 19959–19965, Feb. 2025, https://doi.org/10.48084/etasr.9094.

[27] S. Masalmeh, S. A. Farzaneh, M. Sohrabi, M. S. Ataei, and M. Alshuaibi, "A Systematic Experimental Study to Understand the Performance and Efficiency of Gas Injection in Carbonate Reservoirs," *SPE Reservoir Evaluation & Engineering*, vol. 26, no. 4, pp. 1159–1174, Nov. 2023, https://doi.org/10.2118/200057-PA.

[28] B. Khussain *et al.*, "Numerical Simulation of CO2 Storage Potential with Enhanced Sedimentary Basin Characterization: A Case Study in Kazakhstan," *Engineering, Technology & Applied Science Research*, vol. 15, no. 5, pp. 28179–28193, Oct. 2025, https://doi.org/10.48084/etasr.13316.

[29] J. Iskandarov, S. Ahmed, G. S. Fanourgakis, W. Alameri, G. E. Froudakis, and G. N. Karanikolos, "Predicting and optimizing CO_2 foam performance for enhanced oil recovery: A machine learning approach to foam formulation focusing on apparent viscosity and interfacial tension," *Marine and Petroleum Geology*, vol. 170, Dec. 2024, Art. no. 107108, https://doi.org/10.1016/j.marpetgeo.2024.107108.

[30] M. M. A. Awan and F. U. D. Kirmani, "CO_2 injection for enhanced oil recovery: Analyzing the effect of injection rate and bottom hole pressure," *Petroleum Research*, vol. 10, no. 1, pp. 129–136, Mar. 2025, https://doi.org/10.1016/j.ptlrs.2024.08.006.

[31] S. Prakash, D. Joshi, K. Ojha, and A. Mandal, "Enhanced Oil Recovery Using Polymer Alternating CO2 Gas Injection: Mechanisms, Efficiency, and Environmental Benefits," *Energy & Fuels*, vol. 38, no. 7, pp. 5676–5689, Apr. 2024, https://doi.org/10.1021/acs.energyfuels.3c04258.

[32] B. Ratov *et al.*, "Identifying the operating features of a device for creating implosion impact on the water bearing formation," *Eastern-European Journal of Enterprise Technologies*, vol. 5, no. 1 (125), pp. 35–44, Oct. 2023, https://doi.org/10.15587/1729-4061.2023.287447.

[33] N. Tileuberdi, B. Nassibullin, A. Yskak, and I. Gussenov, "Permeability Damage Induced by Low and High Molecular Weight Polymer Gels in Porous Media," *Engineered Science*, no. 29, Jan. 2024, Art. no. 1092, https://doi.org/10.30919/es1092.

[34] B. Orinbaev *et al.*, "Comprehensive Use of Electrical Inverse Lateral and Radioactive Logging for Strata Properties Investigation in Cased Wells," *ES Materials and Manufacturing*, vol. 27, 2025, Art. no. 1417, http://doi.org/10.30919/mm1417.

[35] B. T. Ratov, R. Y. Bayamirova, V. L. Khomenko, E. A. Kazimov, and A. R. Togasheva, "Determination of the composition and static characteristics of a water shutoff agent for the Kalamkas field," *SOCAR Proceedings*, no. 1, pp. 67–76, 2025, https://doi.org/10.5510/OGP20250101045.

[36] M.-X. Bai, Z.-C. Zhang, E.-L. Yang, and S.-Y. Du, "Experimental study of microscopic oil production and CO2 storage in low-permeable reservoirs," *Petroleum Science*, vol. 22, no. 2, pp. 756–770, Feb. 2025, https://doi.org/10.1016/j.petsci.2024.12.015.